RESEARCH INTO FAULT MOTION IN SICHUAN-YUNNAN REGION, CHINA INCORPORATING EARTHQUAKE RISK ANALYSIS

Guojie Meng[1], Jinwei Ren[1], Zhengkang Shen[2], Min Wang[1], Weijun Gan[2], Qi Wang[3], Xuejun Qiao[3]

[1]Institute of Earthquake Science, China Earthquake Administration, Beijing, China
[2]Institute of Geology, China Earthquake Administration, Beijing, China
[3]Institute of Seismology, China Earthquake Administration, Wuhan, China
Email: mgj@seis.ac.cn mengguojie@sina.com

ABSTRACT :

We have analyzed the characteristics of main faults in terms of slip rates in Sichuan-Yunnan region, China based on GPS measurements in the period of 1997-2007. Dividing the study area into 12 tectonic blocks separated by faults suggested by geological investigation, we derived the Euler vectors of individual blocks and relative Euler vectors of block-pair for adjoining blocks by GPS velocity of GPS stations throughout. The slip rates of individual active faults were calculated, and their motion styles were analyzed in detail. We find that the linking section between the Xianshuihe and the Anninghe fault appears sharp motion variation, possibly implying high seismic risk there. Besides southwestern portion of Longmenshan fault also needs much attention to be paid on due to the great impact by the quick slip of Xianshuihe fault.

KEYWORDS: Fault activity, tectonic block, Sichuan-Yunnan region, earthquake risk analysis

1. INTRODUCTION

Sichuan-Yunnan region is very active tectonically and seismically. It lies within the broadest and most active area of intra-continental deformation. Several major active faults are present there(Figure 1). The Xianshuihe fault, the Red River fault, the Xiaojiang fault and the Jinshajiang fault outline a diamond-shaped tectonic block, named as the Sichuan-Yunnan rhombic tectonic block (Kan et al., 1977). In order to study the crustal deformation and its process, Some GPS station were established throughout this region and several preliminary results were obtained (King et al., 1997; Chen et al., 2000; Shen, et al., 2005), however the explanation of tectonics in this region is not yet convincing because of sparse data. In order to obtain more detailed active regime and accurate investigation of fault motions, much denser GPS stations are quite needed. Under the financial support of the project of Dynamic Process and Strong Earthquake Prediction of Block Boundaries, we construct totally 76 GPS stations in 2005 in west Sichuan region(Figure 2), of which 6 stations are continuously operating, 70 stations are campaigned and were occupied thrice in the period of 2005-2007, once per year. We combined measurements available for all GPS stations in Sichuan-Yunnan region to show the pattern of fault and block motions and to shed new insights on the dynamics of the contemporary tectonic deformation there.

2. SEISMOTECTONIC SETTING

Both the Xianshuihe fault, at the northern end of the rhombic tectonic block and the Xiaojiang fault at eastern end are left-lateral striking-slip fault. Red river fault, marking the southwestern end of it, is a right-lateral strike-slip fault. Along the Xianshuihe Fault, the annual rate of slip since the Quaternary is about 8-15mm/yr (Deng, et al., 1994; Xu, et al., 2003). Historically, a series of large earthquakes occurred along this fault, in particular on the Luohuo-Daofu segment as follows: 1816 earthquake of M 7.5, the 1893 earthquake of M 7, the 1923 earthquake of M 7.3, and the 1981 earthquake of Ms 7.0 (Yang et al.2005).To the northeast of rhombic tectonic block is the 470km long, NE striking Longmenshan fault, which rises to 6500m, shows little evidence of recent shortening. The Longmenshan fault frequently ruptures in small to moderate size earthquakes, but no earthquake with

M ≥7 have been documented along fault prior to the recent Ms8.0 event. Some earthquakes with magnitudes around 6 occurred here historically, such as the 1657 Wenchuan earthquake of Magnitude of M6.5 and the 1970 Dayi earthquake of Ms 6.2. Along Xiaojiang Fault, the rate of slip since the Quaternary is about 6.4-8.8mm/yr (Su and Qin, 2001), and several strong earthquakes, including the 1833 Songming earthquake of Magnitude of M8, and 1966 Dongchuan earthquake of Ms6.5. Along the Red River fault, the slip rate since the Quaternary is about 4-6mm/yr on the northern segment, and 7-9mm/yr on the southern segment of the fault (Guo, et al., 1984).

Previous studies indicate that some of the larger earthquakes of the region occurred along these major fault systems, both historically and recently. The large earthquake with M≥7 took place mainly along active faults and contributed in many cases, to their formation(Deng, 1994). Strong earthquakes occurred frequently along the Red River Fault in historical times. Among the most important historical events are the 1925 Dali earthquake of Ms7.0 and the instrumental 1970 Tonghai earthquake of Ms 7.8 that ruptured the northwestern and southeastern parts of the Red River fault, respectively. Focal mechanisms of earthquakes bounding the tectonic block reveal a NNE horizontal maximum compressive stress for the region suggesting a relative movement of the block to the SEE (Xu, et al, 1989).

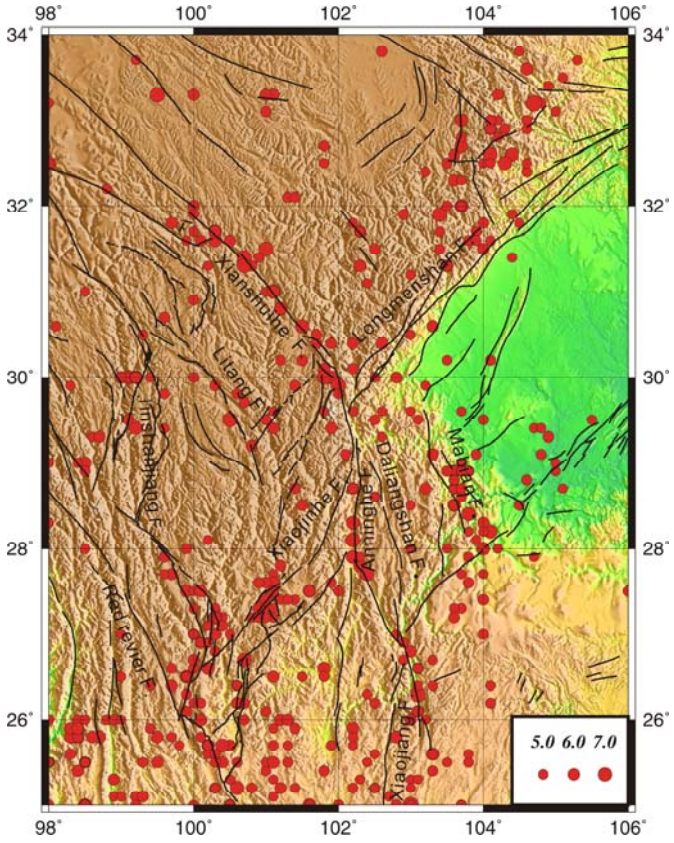

Figure 1. Seismosetting of Sichuan-Yunnan area

3. GPS DATA PROCESSING

The GPS data are processed in three steps. Firstly GAMIT software is used to for single-day solutions (King and Bock, 2003). Regional station coordinates, satellite state vectors, 11 tropospheric zenith delay parameters per site and day, and phase ambiguities are solved. IGS final orbits and IERS Earth Orientation Parameters are used, and elevation-depend antenna phase center corrections are made, following the tables recommended by the IGS. 16 global IGS stations are used to serve as ties with ITRF2005 (Altamimi, et al., 2007). Secondly the least square adjustment vector and the variance-covariance matrix for station positions and orbital elements estimated for each independent daily solution are then combined with global H-files from Scripps Institution of Oceanography (SIO) by the GLOBK software (Herring, 2002). Common parameters in all solutions, such as the satellite orbit, polar motions, and tracking station positions, are solved with loose constraints on all the parameters. In

the final step, station positions and velocities are estimated with the QOCA software (Dong et al., 1998). The QOCA modeling of the data is done through sequential Kalman filtering, allowing adjustment for global translation and rotation of each daily solution and minimizing the positions and velocities of IGS core stations with respect to ITRF2005. We impose the reference frame by minimizing the position and velocity deviations of ~40 IGS core stations with respect to the ITRF2005 while estimating an orientation, translation, and scale transformation. Random walk perturbations are allowed for some parameters whose errors are found correlated with time. The height coordinates and vertical velocities are weighted by a factor of 10 less than the horizontal components.

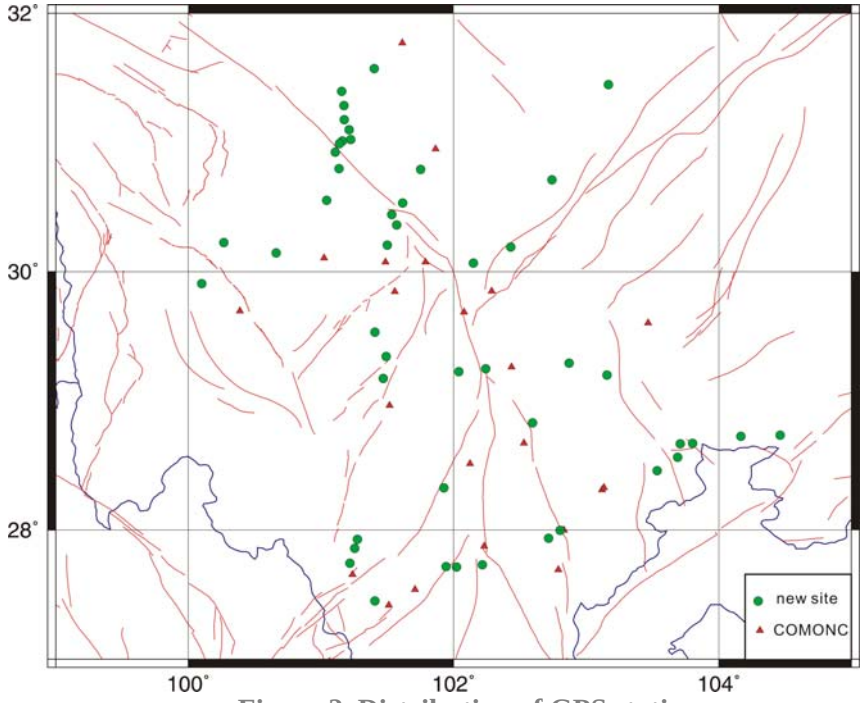

Figure 2. Distribution of GPS stations

4. RESULTS

We derive a detailed horizontal velocity field for West Sichuan-Yunnan area using GPS data collected from the Crustal Motion Observation Network of China and the newly established network supported by the project of Dynamic Process of Boundaries of Active Tectonic Blocks and Prediction of Strong Earthquakes between 1998-2007. For further analysis of block motion and fault activity, we assigned all GPS site to individual tectonic blocks and determined the Euler vectors of blocks using the velocities of GPS stations in the stable interior of them.

4.1 block motion

We assume that upper crustal deformation is block-like. Sichuan-Yunnan region is divided into rigid blocks, which move relative to each other in the form of translation and rotation. These blocks are delineated by active faults, which absorb the deformation associated with relative block motions. Elastic deformation along block boundaries are not taken into consideration, since approximately 70% and 80% of elastic deformation take place within 30km of a strike-slip fault locked at 10 and 15 km depth respectively [e.g., Savage and Burford, 1970]. We derive the Euler vectors of 12 tectonic blocks by performing an iteration procedure. We first compute a common angular velocity pole of all stations located in individual blocks. We then eliminate potential stations not consistent with rigid assumption from the total station velocities through the iteration procedure, each time deleting a site with the largest post-fit residual, until all the postfit residual velocities are within 1 mm/yr. The Euler vectors of all 12 tectonic blocks are listed in see Table. Besides we obtained the translation rate for individual blocks by computing average rate for the sites left after the above iteration process.

Table1. Microblock Motion With Respect to the Eurasia Platea

Microblock	WRMS (mm/yr)	Lon (°)	Lat (°)	Angular Velocity (°/myr)	Ve (mm/yr)	Vn (mm/yr)	Number of sites
Longmenshan	0.37	264.2±11.8	9.8±29.0	0.1089±0.0837	7.8±0.4	-3.9±0.4	13
ANH-DLS	0.50	98.3±6.7	24.1±1.5	-1.171±0.318	9.8±0.8	-8.6±0.8	5
Central Yunan	0.44	97.3±1.5	23.3±0.2	-1.304±0.086	7.2±0.4	-12.8±0.4	17
East Yunnan	0.46	117.7±10.8	39.3±3.3	0.232±0.038	7.2±0.4	-4.1±0.4	13
East Tibet	0.43	96.2±0.80	26.2±0.1	-2.393±0.105	16.7±0.6	-5.9±0.6	8
LJ-ANNH	0.16	106.5±15.5	30.9±1.8	1.654±0.697	9.8±0.7	-12.7±0.7	2
NE Sichuan	0.38	141.4±36.4	59.8±7.8	0.120±0.025	7.2±0.3	-4.2±0.3	23
Shangrila	0.13	94.0±3.5	21.4±2.5	-0.945±0.218	14.9±0.7	-10.1±0.7	4
South China	0.45	188.9±28.7	64.2±2.2	0.085±0.010	7.2±0.3	-4.2±0.2	38
West Mabian	0.19	117.7±36.0	45.8±12.0	0.226±0.112	6.7±0.6	-4.8±0.6	3
Yajiang	0.31	95.3±1.2	24.2±0.5	-1.222±0.078	12.7±0.4	-12.0±0.4	11
Yinzhi	0.50	98.0±1.8	22.7±0.1	-1.557±0.129	1.0±0.5	-8.3±0.5	10

[a] Minus represents clockwise rotation, positive value denotes anti-clockwise rotation for angular velocities.

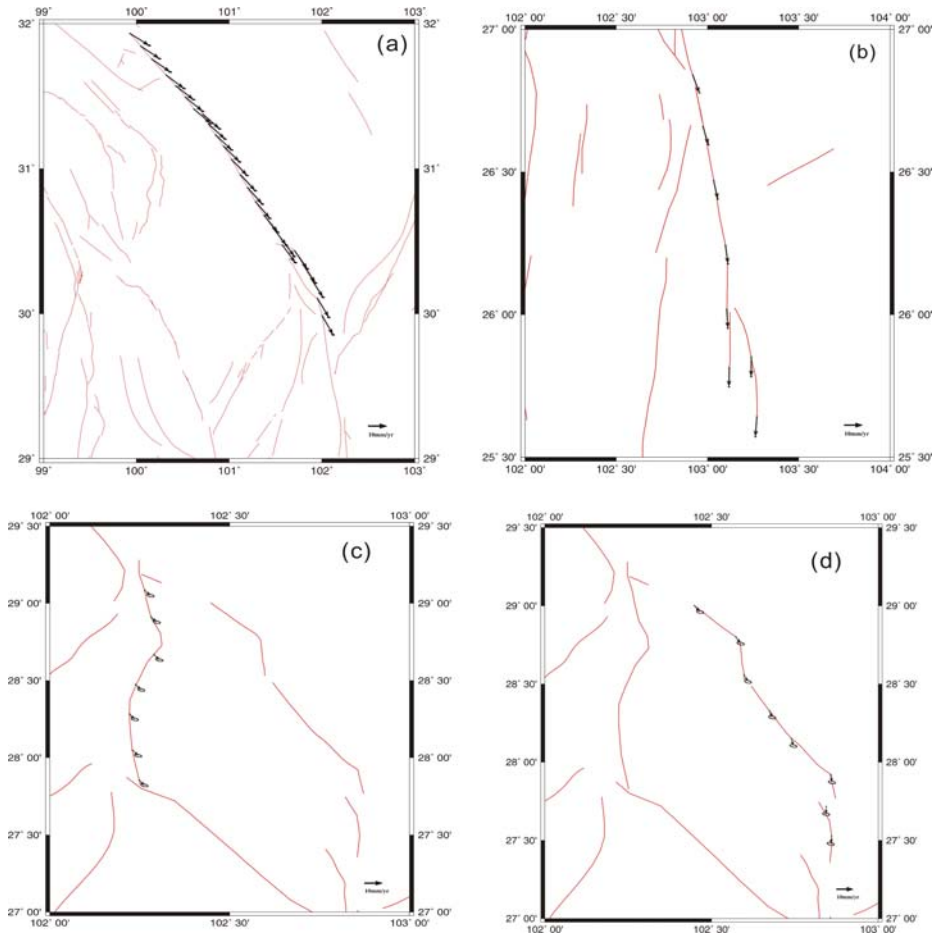

Figure 3. Examples of slip rate of active faults

4.2 Fault motion

We estimate relative Euler vectors of block-pair by taking difference of the adjoining blocks and further calculated the slip rates for individual faults. Our results reveal that north segment of Xianshuihe fault exhibits a left slip of 7.2±0.7mm/yr and compression rate of 3.0±0.5mm/yr, and south segment slips left laterally at a rate of 9.3±0.5mm/yr, with extension of 1.4±0.2mm/yr(see Figure 3), consistent with previous investigations [Chen, et al., 2000; Shen, et al., 2005]. Longmenshan fault shows very small motion, with left slip rate of 1.0±0.2mm/yr and compression rate of 0.3±0.3mm/yr. Since great impact by the quick slip of Xianshuihe fault, southwestern portion of Longmenshan fault perhaps is a domain

of high seismic risk.

No significant fault-normal motion is detected across Litang fault, but it shows compression of 2.8±0.3mm/yr. We find right-lateral slips across the north and south sections of Lijiang-Xiaojinhe fault at rates of 2.8±0.3mm/yr and 5.3±1.9mm/yr, compression rates 5.0±0.5mm/yr and 6.3±1.0mm/yr respectively. We determine 4.0±0.9 mm/yr of left slip across both Anninghe and Dalingshan faults with little extension. Linking a right step between the Anninghe and Xiaojiang fault, Zemuhe fault slips left laterally at a rate of 7.6±0.7mm/yr and extends at a rate of 4.1±1.4.mm/yr. The Xiaojiang fault shows little fault-normal motion but a left slip of 8.7±0.7mm/yr. Deformation across Mabian fault is not significant at 95% confidence level at present time. Since the linking section between the Xianshuihe and the Anninghe faults appears sharp motion variation, it possibly implies a high earthquake risk there.

5 CONCLUDING REMARK

The characteristics of main faults in terms of slip rates in Sichuan-Yunnan region, China were analyzed based on GPS measurements in the period of 1997-2007. The Euler vectors of individual blocks and relative Euler vectors of block-pair for adjoining blocks are derived from the GPS velocity field and the slip rates of individual faults are obtained. Our result shows that Xianshuihe fault is most active in this region with left-lateral slip rate of 7.2±0.7mm/yr at northwestern segment and 9.3±0.5mm/yr at southeastern portion. The Longmenshan fault underwent relatively small slip rate of ~1mm/yr prior to the tragic Ms 8.0 earthquake of 12 May, 2008. Considering that the linking section between the Xianshuihe and the Anninghe faults appears sharp motion variations, possibly suggesting high earthquake risk recently there. In addition, southwestern portion of Longmenshan fault perhaps is also thought as a domain of high seismic risk due to impact by quick slip of the southeastern segment of Xianshuihe fault.

REFERENCES

Allen, C. R., Luo, Z., Qian, H., Wen, X., Zhou, H. and Huang W. (1991). Field study of a highly active fault zone: The Xianshuihe fault of south-western China, *Geol. Soc. Am. Bull.*, 103, 1178-1199.

Altamimi, Z., Collilieux, X., Legrand, J., Garayt, B. and Boucher C. (2007). ITRF2005: a new release of the International Terrestrial Reference Frame based on time series of station positions and Earth Orientation Parameters, *J. Geophys. Res.*, 112(B09401), doi:10.1029/2007JB004949.

Chen, Z., Burchfiel, B. Liu,Y., King, R., Royden, L., Tang, W., Wang, E., Zhao, J., and Zhang X. (2000). Global Positioning System measurements from eastern Tibet and their implications for Inida/Eurasia intercontinental deformation, *J. Geophys. Res.*, 105, 16, 215-16,227.

Deng, Q., Xu X. and Yu, G. (1994). Characteristics of regionalization of active faults in China and their genesis, In : Active Fault Research in China, Department of Science and Technology, State Seismological Bureau of China, 1-14.

England, P., and Molnar, P. (2005). Late Quaternary to decadal velocity fields in Asia, *J. Geophys. Res.*, 110, B12401, doi:10.1029/2004JB0003541.

Guo, S., Zhang, J., Li, X., Xiang, H., Chen, T. and Zhang, G. (1984). Fault displacement and recurrence intervals of earthquakes at the northern segment of Honghe fault zone, *Seismology and Geology*,6,1-12

Herring, T. A., (2002). *GLOBK, Global Kalman filter VLBI and GPS analysis software*, Mass. Inst. of Tech., February 15.

Kan, R., Zhang, S., Yan F. and Yu, L.(1977). Present tectonic stress and its relation to the Characteristics of recent tectonic activity in southwestern China, *Acta Geophsica Sinica, 20(2)*,96-109.

King, R., Shen, F., Burchfiel, B., Chen, Z., Li, Y., Liu, Y., Royden, H., Wang, E., Zhang, X. and Zhao J. (1997).Geodetic measurement of Crustal motion in southwest China, *Geology*, 25, 179-182.

King, R. W. and Bock, Y. (2003).*Documentation for the GAMIT GPS Analysis software*, Mass. Inst. of Tch., Scripps Inst. Occeangr., Release 10.1, November 11.

Savage, J. C. and Burford, R. O. (1970). Accumulation of tectonic strain in California, Bull. *Seismol. Soc. AM.*, 60, 1877-1896.

Shen, Z., Lü,J., Wang, M. and Bürgmann, R.(2005). Contemporary crustal deformation around the southeast borderland of the Tibetan Plateau, *J. Geophys. Res.*, 110, B11409,

doi:10.1029/2004JB003421.
Su, Y., and Qin, J., (2001). Strong earthquake activity and relation to regional neo-tectonic movement in Sichuan-Yunnan region. *Earthq. Res. China*, 17(1):24-34.
Yang, Z., Waldhauser, F., Chen, Y. and Richard, P. (2005). Double-difference relocation of earthquake in Cenral-western China, *Journal of Seismology*, 9:241-264.
Xu, X., Wen, X., Zheng, R., Ma, W., Song, F. and Yu, G. (2003). Pattern of latest tectonic motion and its dynamics for active blocks in Sichuan-Yunnan region, China, *Sci. China, suppl.*, 210-226.
Xu, Z., Wang, S., Huang, Y. and Gao, A.(1989). The tectonic stress field of Chinese continent deduced from a great number of earthquake. *Acta Geophysica Sinica*, 32(6), 636-647.
Zhang, P., et al.(2004), Continuous deformation of the Tibetan Plateau from global positioning system data, *Geology*, 32, 809-812.

ACKNOWLEDGMENTS.
We are grateful to the Institute of Surveying and Mapping, Sichuan Sichuan Earthquake Administration in organizing all GPS monuments establishments and field measurements.